Proceedings of the ASME 2014 International Design Engineering Technical Conferences & Computers and Information in Engineering Conference
IDETC/CIE 2014
August 17-20, 2014, Buffalo, New York, USA

DETC2014-34430

EFFECTS OF DNA ENCAPSULATION ON BUCKLING INSTABILITY OF CARBON NANOTUBE BASED ON NONLOCAL ELASTICITY THEORY

Jacob Rafati *
Mechanical Engineering
University of California, Merced
Merced, California 95348
Email: jrafatiheravi@ucmerced.edu

Mohsen Asghari
Mechanical Engineering
Sharif University of Technology
Tehran, Iran
Email: asghari@sharif.edu

Sachin Goyal
Mechanical Engineering
University of California
Merced, California 95348
Email: sgoyal2@ucmerced.edu

ABSTRACT

Carbon nanotubes (CNTs) are capable to absorb and encapsulate some molecules to create new hybrid nano-structures providing a variety of functionally useful properties. CNTs functionalized by encapsulaitng single-stranded deoxy-ribonucleic acid (ssDNA) promise great potentials for applications in nanotechnology and nano-biotechnology. In this paper, buckling instability of ssDNA@CNT i.e. hybrid nano-structure composed of ssDNA encapsulated inside CNT has been investigated using the nonlocal elasticity theory. The nonlocal elasticity theory is capable to capture the small scale effects due to the discontinuity of nano-structures at atomic scales. The nonlocal elastic rod and shell equations are derived for modeling ssDNA and CNT respectively. Providing numerical examples, it is predicted that, ssDNA@(10,10) CNT is more resistant than the pristine (10,10) CNT against the buckling instability under radial pressure due to the inter-atomic van der Waals interactions between DNA and CNT. Furthermore, nonlocal elasticity theory predicts lower critical buckling pressure than does the local elasticity theory.

1. INTRODUCTION

Carbon nanotubes (CNTs) are 4^{th} allotrope of carbon with a graphitic hexagonal lattice [1] and since CNTs have hollow cylindrical shape, they are capable to absorb and encapsulate atoms and small molecules [2] and nano-structures such as C_{60} fullerenes [3], linear carbon chain (C-chain) [4] and single-stranded DNA (ss-DNA) [5, 6]. The inter-atomic van der Waals (vdW) interaction between encapsulated material and CNT plays the main role in the insertion and encapsulation process [6, 7]. Encapsulation is one of the alternative ways for "functionalization" of CNT by creating a new hybrid nano-structure. In particular, encapsulation alters the physical, electrical and mechanical characteristics of CNT [6, 8, 9] providing for new functional capabilities. Carbon nanotubes functionalized with other materials, specially biological species have been developed for biomedical and biotechnological applications, including drug delivery, enzyme immobilization and DNA transfection [6], for applications in manufacturing of nano-electronic devices [10], probes and sensors [6, 11] and for applications in nano-robotics [12]. In many of these applications, the functionalized CNTs are subjected to mechanical loading. The molecular dynamic (MD) simulations predicts that carbon nanotubes and their hybrid nano-structures are highly elastic [13] and buckle under high stress for various mechanical loading scenarios, such as axial compression [14], torsional moment [15], external radial pressure [16] and bending moment [17]. Analysis of how encapsulation alters the buckling behavior has gained recent attention in the fast-growing research field of functionalized CNTs. For example, the encapsulation of C_{60} fullerenes inside (10,10) CNT, which occurs spontaneously results in a hybrid nano-structure that is more resistant to buckling than is the pristine CNT as predicted by both MD simulations and continuum theory [13–15, 17–19]. Similar behavior has been predicted from MD simulations and

*Address all correspondence to this author. This work is part of author's master thesis project at Sharif University of Technology, Tehran, Iran.

continuum theory for nanowires, which are hybrid nano-structure with C-Chains encapsulated into CNT, under various mechanical loading scenarios [20, 21].

Although MD simulations are suitable for investigating the mechanical characteristics of nano-structures, they are time-consuming and computationally expensive for large-sized systems. Continuum theories on the other hand have recently provided very efficient tools to simulate and analyze the dynamics of several nano-structures. For example, the models of CNT based on shell theory successfully predict their dynamic behavior in deformation including onset of buckling instability under axial loading [22, 23], uniform external pressure [24], bending [25] and torsional moments [26]. Likewise, thin filament models based on elastic rod theory are evolving to simulate bending and twisting deformations of DNA [27–29] including looping [30–33] and supercoiling due to torsional buckling [34, 35].

While most of the continuum models make simplistic course-grained approximations, efforts are underway to develop methods for deriving constitutive laws for continuum approximations directly from MD simulations [36–39]. In several nano-structure applications, however, the spacing between atoms can be significant relative to the length scale of deformation of interest. Hence, the conventional continuum theories that are based on the philosophy of the structural continuity can still be inaccurate. The "nonlocal elasticity theory" introduced by Eringen [40, 41] overcomes this inaccuracy by taking the small scale effects of the structural discontinuity into account empirically in the constitutive law. The continuum models of CNTs based on nonlocal elasticity are therefore more accurate [42–45] than the conventional local elasticity theory. The nonlocal elastic shell model has been used for CNTs to analyze buckling instability under radial pressure [46], axial loading [47], and torsional moment [48], and to analyze thermal buckling instability [49], vibration behavior [50] and the wave propagation [51]. It is noteworthy that nonlocal elasticity predicts less resistance to buckling than does the local elasticity [18, 19, 45, 46, 48, 49].

In this paper, we employ the nonlocal elasticity theory to investigate the buckling instability of a special type of hybrid nano-structure ssDNA@SWCNT, which is single-walled carbon nanotube (SWCNT) encapsulated with a single-stranded deoxyribonucleic acid (ssDNA). Section 2 begins with reviewing the nonlocal elasticity theory and the nonlocal shell model that we use for SWCNT. We next introduce the nonlocal elastic rod model for ssDNA in Section 2. In section 3, we derive the continuum representation for atomic interaction between encapsulated ssDNA and SWCNT as distributed force on ssDNA and internal vdW pressure on SWCNT. Then we substitute these force and pressure interactions in nonlocal shell and rod models described in section 2 to derive naturally coupled equations governing the stability of ssDNA@CNT in section 4. Then we use the governing equations to investigate the buckling of the hybrid nano-structure under uniform external radial pressure. We also derive eigen-value formulation to calculate the critical pressure for the onset of radial buckling in terms of all axial and circumferential buckling modes. In section 5, we present results illustrating the applicability of the nonlocal models for predicting the critical pressure for special hybrid ssDNA@(10,10) CNT and also the effect of encapsulated ssDNA in the hybrid nano-structure compared with pristine (10,10) CNT, and finally we verify the predictions of our model with existing results based on MD simulations and continuum theory in similar phenomena for other categories of hybrid nano-structures such as one specific nanopeadpod (C_{60}@(10,10) SWCNT) [13–15, 17–19] and also (5,5) and (0,9) nanowires [20, 21].

2. NONLOCAL ELASTIC MODELS

2.1. Constitutive Law in Nonlocal Elasticity Theory

In the conventional theory of local elasticity, the stress tensor σ at a material point $\mathbf{x}$ of a continuous body is a function of the strain tensor ε at that point $\mathbf{x}$ only and has no explicit dependence on neighboring material points i.e."nonlocal points". This assumption breaks down at the length scales of inherent discreteness of nano-structures. This discrepancy is circumvented in the nonlocal elasticity theory introduced by Eringen [40, 41], in which stress tensor σ at a material point explicitly depends on to strain tensor field ε not only at that point but also at the surrounding points in the body Ω with appropriate weight distribution. The constitutive equation for nonlocal elasticity theory has been suggested by Eringen [41] in the integral form as:

$$\sigma(\mathbf{x}) = \iiint_{\Omega} \Gamma(|\mathbf{x}' - \mathbf{x}|, \tau)\ \mathbf{C} : \varepsilon(\mathbf{x}')\, \mathrm{d}V. \tag{1}$$

Here, $\Gamma(|\mathbf{x}' - \mathbf{x}|, \tau)$ is weight distribution, also called nonlocal modulus and $|\mathbf{x}' - \mathbf{x}|$ is the distance between a local point $\mathbf{x}$ and a nonlocal point $\mathbf{x}'$. $\mathbf{C}$ denotes the fourth order elasticity tensor and the colon ":" in $\mathbf{C} : \varepsilon$ stands for double contraction. Also $\tau = e_0 a/l$, where a is the internal characteristic length (e.g. bond lengths), l is the external characteristic length (e.g. structural length), and e_0 as a material parameter empirically determined for a nanostructure to make an agreement between experimental measurements and continuum model predictions [41, 42, 49, 51]. By assuming appropriate Γ, Eringen developed the differential form of nonlocal constitutive equation based on integral form in Eqn. (1) as [41, 49]:

$$(1 - \eta^2 \nabla^2)\, \sigma = \mathbf{C} : \varepsilon, \tag{2}$$

where $\eta = \tau l = e_0 a$ is referred to as the small scale coefficient [49, 51] and ∇^2 is the Laplacian operator. Recognizing that $\nabla \sim 1/l$, note that when the internal characteristic length is negligible with respect to the external characteristic length, i.e. when

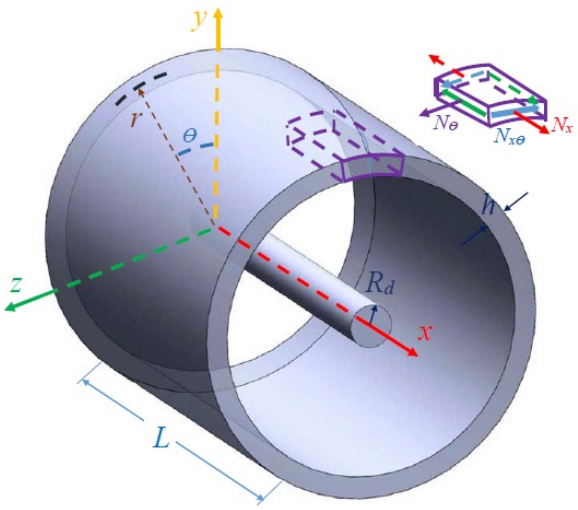

FIGURE 1. Schematic of Rod-Shell model for ssDNA@SWCNT.

$\eta/l \to 0$, the nonlocal constitutive law Eqn. (2) approaches the familiar constitutive law in local elasticity theory $\sigma = \mathbf{C} : \varepsilon$.

2.2. Nonlocal Elastic Shell Model

This section reviews the Donnell's nonlocal shell model that is extensively developed in [19,46,49]. Consider a hollow cylindrical shell with length L, mean radius R and thickness h as shown in Fig. 1. Let (x,θ,r) be the axial, circumferential and radial coordinates of any material point of the shell in the reference configuration and $\mathbf{u} = (u_1,u_2,u_3)$ be the displacement field of the shell along these coordinates. Based on the Donnell's assumptions for thin shells, $\mathbf{u}$ is given by [52]:

$$\mathbf{u} = \begin{Bmatrix} u_1 \\ u_2 \\ u_3 \end{Bmatrix} = \begin{Bmatrix} u(x,\theta) - (r-R)\frac{\partial w}{\partial x} \\ v(x,\theta) - \frac{r-R}{R}\frac{\partial w}{\partial \theta} \\ w(x,\theta) \end{Bmatrix}, \tag{3}$$

where (u,v,w) denotes displacement field of the mid-surface i.e. cylindrical surface at $r = R$ in Fig. 1.

The radial normal stress σ_r is neglected in comparison to σ_x and σ_θ. Substituting displacement field given by Eqn. (3) into $\varepsilon_{ij} = \frac{1}{2}(u_{i,j} + u_{j,i})$, the components of strain tensor ε are obtained as:

$$\varepsilon_x = u_{1,x} = u_{,x} - (r-R)w_{,xx}, \tag{4a}$$

$$\varepsilon_\theta = \frac{u_{2,\theta}}{R} = \frac{v_{,\theta}}{R} + \frac{w}{R} - \frac{r-R}{R^2}w_{,\theta\theta}, \tag{4b}$$

$$\gamma_{x\theta} = \frac{u_{1,\theta}}{R} + u_{2,\theta} = \frac{u_{,\theta}}{R} + v_{,x} - 2\frac{r-R}{R}w_{,x\theta}, \tag{4c}$$

where $u_{,x} = \partial u/\partial x$ and so on. From Eqn. (2), the nonlocal constitutive law for isotropic material is

$$(1-\eta^2\nabla^2)\begin{Bmatrix} \sigma_x \\ \sigma_\theta \\ \tau_{x\theta} \end{Bmatrix} = \frac{E}{1-\nu^2}\begin{Bmatrix} \varepsilon_x + \nu\varepsilon_\theta \\ \nu\varepsilon_x + \varepsilon_\theta \\ \frac{1-\nu}{2}\gamma_{x\theta} \end{Bmatrix}, \tag{5}$$

where E is elastic Young's modulus, ν is the Poisson's ratio and the Laplacian operator $\nabla^2 = \frac{\partial^2}{\partial x^2} + \frac{1}{R^2}\frac{\partial^2}{\partial \theta^2}$. The axial, circumferential and shearing forces $(N_x, N_\theta, N_{x\theta})$ per unit length due to corresponding stress components are defined as [49]:

$$\begin{Bmatrix} N_x \\ N_\theta \\ N_{x\theta} \end{Bmatrix} = \int_{R-h/2}^{R+h/2} \begin{Bmatrix} \sigma_x \\ \sigma_\theta \\ \tau_{x\theta} \end{Bmatrix} \mathrm{d}r. \tag{6}$$

Substituting Eqn. (4) in (5) and the result into (6), we get

$$(1-\eta^2\nabla^2)\begin{Bmatrix} N_x \\ N_\theta \\ N_{x\theta} \end{Bmatrix} = K\begin{Bmatrix} u_{,x} + \frac{\nu}{R}(v_{,\theta} + w) \\ v_\theta/R + w/R + \nu u_{,x} \\ \frac{(1-\nu)}{2}(u_{,\theta}/R + v_{,x}) \end{Bmatrix}, \tag{7}$$

where $K = Eh/(1-\nu^2)$ is called the effective axial stiffness. Similarly, the resultant moments per unit length $(M_x, M_\theta, M_{x\theta})$ due to corresponding stress components are defined as [49]:

$$\begin{Bmatrix} M_x \\ M_\theta \\ M_{x\theta} \end{Bmatrix} = \int_{R-h/2}^{R+h/2} \begin{Bmatrix} \sigma_x \\ \sigma_\theta \\ \tau_{x\theta} \end{Bmatrix} (r-R)\,\mathrm{d}r. \tag{8}$$

Substituting Eqn. (4) in (5) and the result into (8), we get

$$(1-\eta^2\nabla^2)\begin{Bmatrix} M_x \\ M_\theta \\ M_{x\theta} \end{Bmatrix} = -D\begin{Bmatrix} w_{,xx} + \nu w_{,\theta\theta}/R, \\ w_{,\theta\theta}/R^2 + \nu w_{,xx}, \\ \frac{(1-\nu)}{R}w_{,x\theta}, \end{Bmatrix}, \tag{9}$$

where $D = Eh^3/12(1-\nu^2)$ is called the effective bending stiffness of the shell [46,49]. The linearized equations of equilibrium for the shell element in terms of the resultant forces and moments

per unit length are [52]:

$$N_{x,x}+\frac{1}{R}N_{x\theta,\theta}=0, \tag{10}$$

$$N_{x\theta,x}+N_{\theta,\theta}=0, \tag{11}$$

$$\begin{aligned}Q_{xr,x}+\frac{1}{R}Q_{\theta r,\theta}+\frac{\partial}{\partial x}\left(N_x\frac{\partial w}{\partial x}\right)+\frac{1}{R}\frac{\partial}{\partial x}\left(N_{x\theta}\frac{\partial w}{\partial \theta}\right)\\ +\frac{1}{R}\frac{\partial}{\partial \theta}\left(N_{x\theta}\frac{\partial w}{\partial x}\right)+\frac{1}{R}\frac{\partial}{\partial \theta}\left(N_\theta\frac{\partial w}{\partial x}\right)\\ -\frac{N_\theta}{R}-p_{net}=0,\end{aligned} \tag{12}$$

where Q_{xr} and $Q_{\theta r}$ denote the resultant shearing forces in the radial direction and $p_{net}=p_{ext}-p_{int}$ denotes the net external pressure on the shell. The rotational equilibrium of shell element is satisfied when [52]:

$$Q_{xr}=M_{x,x}+\frac{1}{R}M_{\theta x,\theta}, \tag{13}$$

$$Q_{\theta r}=M_{x\theta,x}+\frac{1}{R}M_{\theta,\theta}. \tag{14}$$

Substituting Eqns. (13) and (14), Eqn. (12) can be written in terms of the resultant moments as:

$$M_{x,xx}+\frac{2}{R}M_{x\theta,x\theta}+\frac{1}{R^2}M_{\theta,\theta\theta}+\Psi[w]-\frac{N_\theta}{R}-p_{net}=0, \tag{15}$$

where

$$\Psi[.]=N_x\frac{\partial^2}{\partial x^2}+2N_{x\theta}\frac{1}{R}\frac{\partial^2}{\partial x\partial\theta}+N_\theta\frac{1}{R^2}\frac{\partial^2}{\partial\theta^2} \tag{16}$$

is a differential operator [48,49]. Applying the nonlocal elasticity operator $(1-\eta^2\nabla^2)$ to the equilibrium Eqns. (10, 11, 15) and then substituting the resultant forces and moments from Eqns. (7) and (9), the equilibrium equations in terms of displacement field are obtained as:

$$K\left[u_{,xx}+\nu\frac{v_{x\theta}}{R}+\nu\frac{w_{,x}}{R}+\frac{1-\nu}{2}\left(u_{\theta\theta}+\frac{v_{,x\theta}}{R}\right)\right]=0, \tag{17}$$

$$K\left[\frac{1-\nu}{2}\left(\frac{1}{R}u_{,x\theta}+v_{,xx}\right)+v_{\theta\theta}+\frac{w_{,\theta\theta}}{R^2}+\frac{\nu}{R}u_{,x\theta}\right]=0, \tag{18}$$

$$\begin{aligned}-D\big[w_{,xxxx}+\frac{\nu}{R^2}w_{,xx\theta\theta}+\frac{1}{R^4}w_{,\theta\theta\theta\theta}+\frac{\nu}{R^2}w_{,xx\theta\theta}\\ +\frac{2(1-\nu)}{R^2}w_{,xx\theta\theta}\big]+(1-\eta^2\nabla^2)\Psi[w]\\ -\frac{K}{R}\left(u_{,x}+\frac{\nu}{R}v_{,\theta}+\frac{\nu}{R}w\right)-(1-\eta^2\nabla^2)p_{net}=0.\end{aligned} \tag{19}$$

Eliminating u and v from Eqns. (17)-(19), we arrive at the nonlocal Donnell's equilibrium equation for a tubular shell [48,49]:

$$\begin{aligned}D\nabla^8 w+\frac{Eh}{R^2}\frac{\partial^4 w}{\partial x^4}-(1-\eta^2\nabla^2)\nabla^4\Psi[w]\\ -(1-\eta^2\nabla^2)\nabla^4 p_{net}=0.\end{aligned} \tag{20}$$

Note that by setting $\eta\to 0$, i.e. ignoring the small scale effects, Eqn. (20) will approach the well-known classical Donnell's shell stability equation.

2.3. Nonlocal Elastic Rod Model

Consider a circular rod with length L and radius R_d as Fig 1. The Rod model can sustain axial force F_x, shearing forces (N_y,N_z) , bending moments (M_y,M_z) about both transverse y and z directions and also torsional moment M_x about x direction. Let $\mathbf{u}_d=(u_d^1,u_d^2,u_d^3)$ be displacement field of a point (x,y,z) on the rod. Based on the Euler-Bernoulli beam theory, the displacement field for a rod is given by

$$\begin{Bmatrix}u_d^1\\u_d^2\\u_d^3\end{Bmatrix}=\begin{Bmatrix}u_d(x)+y\frac{\mathrm{d}v_d}{\mathrm{d}x}-z\frac{\mathrm{d}w_d}{\mathrm{d}x}\\v_d(x)\\w_d(x)\end{Bmatrix}, \tag{21}$$

where (u_d,v_d,w_d) is the displacement field of the rod's centerline. Force balance in static equilibrium of a rod element yields

$$F_x(x+\mathrm{d}x)-F_x(x)-f_x\mathrm{d}x=0, \tag{22a}$$

$$N_y(x+\mathrm{d}x)+\left(F_x\frac{\mathrm{d}v_d}{\mathrm{d}x}\right)\Big|_{x+\mathrm{d}x}-N_y(x)-\left(F_x\frac{\mathrm{d}v_d}{\mathrm{d}x}\right)\Big|_x+f_y\mathrm{d}x=0, \tag{22b}$$

$$N_z(x+\mathrm{d}x)+\left(F_x\frac{\mathrm{d}w_d}{\mathrm{d}x}\right)\Big|_{x+\mathrm{d}x}-N_z(x)-\left(F_x\frac{\mathrm{d}w_d}{\mathrm{d}x}\right)\Big|_x+f_z\mathrm{d}x=0, \tag{22c}$$

and the moment balance yields

$$M_x(x+\mathrm{d}x)-M_x(x)=0, \tag{23a}$$

$$M_y(x+\mathrm{d}x)-M_y(x)-N_z\mathrm{d}x=0, \tag{23b}$$

$$M_z(x+\mathrm{d}x)-M_z(x)-N_y\mathrm{d}x=0, \tag{23c}$$

where (f_x,f_y,f_z) are the external distributed forces on the rod per unit length. We assume f_x to be negligible in comparison to f_y and f_z so that F_x is constant. Then, Eqns. (22, 23) reduce to

$$\frac{\partial^2}{\partial x^2}\begin{bmatrix}M_z\\M_y\end{bmatrix}+F_x\frac{\partial^2}{\partial x^2}\begin{bmatrix}v_d\\w_d\end{bmatrix}+\begin{bmatrix}f_y\\f_z\end{bmatrix}=0. \tag{24}$$

Nonlocal constitutive equation from Eqn. (2) is:

$$(1-\eta^2\nabla^2)\,\sigma_x = E_d\,\varepsilon_x, \tag{25}$$

where E_d is the Young's modulus of rod material (i.e. ssDNA), $\nabla^2 = \mathrm{d}^2/\mathrm{d}x^2$ and $\varepsilon_x = u^1_{d,x} = u_{d,x} + yv_{d,xx} - zw_{d,xx}$ is the axial strain. The resultant bending moments (M_y, M_z) due to σ_x over cross section area of the rod is

$$\begin{bmatrix} M_z \\ M_y \end{bmatrix} = \int_A \begin{bmatrix} -y \\ z \end{bmatrix} \sigma_x \,\mathrm{d}A, \tag{26}$$

where A is the cross-section area. Substituting for ε_x from Eqn. (21) in constitutive equation (25) and using Eqn. (26) to eliminate σ_x, we arrive at

$$(1-\eta^2\nabla^2)\begin{bmatrix} M_y \\ M_z \end{bmatrix} = -E_d\,\mathbf{I}\begin{bmatrix} w_{d,xx} \\ v_{d,xx} \end{bmatrix}, \tag{27}$$

where

$$\mathbf{I} = \begin{bmatrix} I_{yy} & 0 \\ 0 & I_{zz} \end{bmatrix} = \begin{bmatrix} \int_A z^2\,\mathrm{d}A & 0 \\ 0 & \int_A y^2\,\mathrm{d}A \end{bmatrix} \tag{28}$$

is the tensor of 2nd moment of the cross section area of the rod, assuming y and z to be the principal bending directions.

Applying the nonlocal elasticity operator $(1-\eta^2\nabla^2)$ to the equilibrium Eqn. (24) and then substituting the resultant moments from Eqn. (27), the equilibrium equations in terms of displacement field are obtained as:

$$\begin{aligned} -E_d I_{zz}\frac{\mathrm{d}^4 v_d}{\mathrm{d}x^4} + F_x\left(\frac{\mathrm{d}^2 v_d}{\mathrm{d}x^2} - \eta^2\frac{\mathrm{d}^4 v_d}{\mathrm{d}x^4}\right) \\ + \left(1-\eta^2\frac{\mathrm{d}^2}{\mathrm{d}x^2}\right) f_y = 0, \end{aligned} \tag{29}$$

$$\begin{aligned} -E_d I_{yy}\frac{\mathrm{d}^4 w_d}{\mathrm{d}x^4} + F_x\left(\frac{\mathrm{d}^2 w_d}{\mathrm{d}x^2} - \eta^2\frac{\mathrm{d}^4 w_d}{\mathrm{d}x^4}\right) \\ + \left(1-\eta^2\frac{\mathrm{d}^2}{\mathrm{d}x^2}\right) f_z = 0. \end{aligned} \tag{30}$$

Note that in this derivation, we ignored the torsional moment M_x, which is expected to be negligible for ssDNA in the buckling analysis of ssDNA@SWCNT.

3. VAN DER WAALS INTERACTIONS

Consider the hybrid nano-structure (ssDNA@SWCNT) composed of a single-strand DNA encapsulated inside an SWCNT with length of L and mid-surface radius R co-axially as seen in Fig. 1. Let U_{vdW} denote the total vdW potential energy stored in ssDNA@SWCNT due to the insertion and encapsulation of ssDNA inside SWCNT, which is the sum of all interatomic vdW potential energy between ssDNA and SWCNT. We assume that U_{vdW} is only dependent on radial distance, r_c from centerline of ssDNA to mid-surface of SWCNT. The Taylor series expansion of U_{vdW} about the initial configuration of ssDNA and CNT i.e. $r_c = R$ is

$$\begin{aligned} U_{vdW} = U_{vdW}(R) + \left.\frac{\partial U_{vdW}}{\partial r_c}\right|_R (r_c - R) + \\ \frac{1}{2}\left.\frac{\partial^2 U_{vdW}}{\partial r_c^2}\right|_R (r_c - R)^2 + \ldots \end{aligned} \tag{31}$$

The equivalent internal vdW pressure distribution p_{vdW} enforced on SWCNT due to the encapsulated ssDNA can be obtained as

$$p_{vdW} = \frac{1}{2\pi RL}\frac{\partial U_{vdW}}{\partial r_c}. \tag{32}$$

The change in distance between ssDNA and SWCNT from the reference configuration can be written as

$$r_c - R = w(x,\theta) - v_d(x)\cos(\theta) - w_d(x)\sin(\theta), \tag{33}$$

recalling that w is the radial displacement of mid-surface points of SWCNT and (v_d, w_d) denotes the displacement of ssDNA in (y,z) directions respectively. Substituting Eqn. (31) and (33) into (32) up to the first order approximation of displacement terms, we obtain the equivalent vdW pressure distribution on SWCNT due to encapsulated ssDNA as

$$p_{vdW} = p_0 - c_d\left[w(x,\theta) - v_d(x)\cos(\theta) - w_d(x)\sin(\theta)\right], \tag{34}$$

where $p_0 = \frac{1}{2\pi RL}\frac{\partial U_{vdW}}{\partial r}\Big|_R$ is the initial vdW pressure on SWCNT %endequation and $c_d = \frac{1}{2\pi RL}\frac{\partial^2 U_{vdW}}{\partial r^2}\Big|_R$ is the vdW pressure coefficient of ssDNA and SWCNT interaction. The vdW reaction force distribution components on ssDNA from SWCNT can be obtained as follows:

$$f_y(x) = \int_0^{2\pi} R p_{vdW}\cos(\theta)\,\mathrm{d}\theta, \tag{35}$$

$$f_z(x) = \int_0^{2\pi} R p_{vdW}\sin(\theta)\,\mathrm{d}\theta, \tag{36}$$

where (f_y, f_z) denote the vdW force on ssDNA per unit length in the transverse y and z directions respectively.

4. EQUATIONS GOVERNING STABILITY OF ssDNA@SWCNT

To analyze buckling of ssDNA@SWCNT, we model ssDNA by nonlocal elastic rod and SWCNT by nonlocal elastic shell described in Section 2, and use the equivalent pressure and force distribution described in Section 3 for vdW non-bonded interaction between ssDNA and SWCNT. Substituting the vdW pressure distribution on SWCNT due to encapsulation of ssDNA from Eqn. (34) into Eqn. (20) and the distributed vdW force on ssDNA from Eqns. (35, 36) into Eqn. (29, 30), stability of hybrid ssDNA@SWCNT is governed by

$$\begin{aligned} D\nabla^8 w + \frac{Eh}{R^2}\frac{\partial^4 w}{\partial x^4} - (1-\eta^2\nabla^2)\nabla^4\Psi[w] \\ +(1-\eta^2\nabla^2)\nabla^4 c_d\,[w - v_d\cos(\theta) - w_d\sin(\theta)] = 0. \end{aligned} \tag{37}$$

$$\begin{aligned} -E_d I_{zz}\frac{\mathrm{d}^4 v_d}{\mathrm{d}x^4} + F_x\left(\frac{\mathrm{d}^2 v_d}{\mathrm{d}x^2} - \eta^2\frac{\mathrm{d}^4 v_d}{\mathrm{d}x^4}\right) \\ +\left(1-\eta^2\frac{\mathrm{d}^2}{\mathrm{d}x^2}\right)Rc_d\left(\int_0^{2\pi} w\cos(\theta)\,\mathrm{d}\theta, -\pi v_d\right) = 0, \end{aligned} \tag{38}$$

$$\begin{aligned} -E_d I_{yy}\frac{\mathrm{d}^4 w_d}{\mathrm{d}x^4} + F_x\left(\frac{\mathrm{d}^2 w_d}{\mathrm{d}x^2} - \eta^2\frac{\mathrm{d}^4 w_d}{\mathrm{d}x^4}\right) \\ +\left(1-\eta^2\frac{\mathrm{d}^2}{\mathrm{d}x^2}\right)Rc_d\left(\int_0^{2\pi} w\sin(\theta)\,\mathrm{d}\theta, -\pi w_d\right) = 0. \end{aligned} \tag{39}$$

These equations are in general coupled due to the vdW interaction between ssDNA and SWCNT, but under some conditions they may be decoupled. For example, assume an Ansatz solution for the radial displacement of CNT, w as a Fourier series:

$$\begin{aligned} w(x,\theta) = &\sum_{m,n} a_{mn}\cos(m\pi x/L)\cos(n\theta) \\ &+\sum_{m,n} b_{mn}\cos(m\pi x/L)\sin(n\theta) \\ &+\sum_{m,n} c_{mn}\sin(m\pi x/L)\cos(n\theta) \\ &+\sum_{m,n} a_{mn}\sin(m\pi x/L)\sin(n\theta), \end{aligned} \tag{40}$$

where m and n are two non-negative integer, and a_{mn}, b_{mn}, c_{mn} and d_{mn} are Fourier series coefficients. Substituting the Ansatz solution, we note that Eqns. (38, 39) are coupled with Eqn. (37) only for $n = 1$, and that there is no coupling between w and (v_d, w_d) for $n \neq 1$.

5. BUCKLING OF ssDNA@SWCNT UNDER RADIAL PRESSURE

In any equilibrium condition having small deformation, the hybrid structure ssDNA@SWCNT under radial pressure must satisfy all the equilibrium equations. If the deformed state is a stable equilibrium, the structure must restore its equilibrium from any arbitrary perturbation. On the other hand, if the equilibrium is unstable, it can be perturbed such that the perturbation grows and the equilibrium is not restored. At critical loading, the equilibrium becomes a neutral equilibrium in linear buckling analysis. Hence, if functions w, v_d and w_d describe the deformation of SWCNT and ssDNA in static equilibrium under the critical radial pressure p_{cr} , and functions $\tilde{w}$, $\tilde{v}_d$ and $\tilde{w}_d$ represent the perturbations which would grow if the radial external pressure exceeds p_{cr}, Eqns. (37)-(39) will also be valid if w, v_d and w_d are replaced with $w+\tilde{w}$, $v_d+\tilde{v}_d$ and $w_d+\tilde{w}_d$. Subtracting the new equations from Eqns. (37-39), the equations governing the stability of hybrid structure in terms of the perturbation functions $\tilde{w}$, $\tilde{v}_d$ and $\tilde{w}_d$ become

$$\begin{aligned} D\nabla^8 \tilde{w} + \frac{Eh}{R^2}\frac{\partial^4 \tilde{w}}{\partial x^4} - (1-\eta^2\nabla^2)\nabla^4\Psi[\tilde{w}] \\ +(1-\eta^2\nabla^2)\nabla^4 c_d\,[\tilde{w} - \tilde{v}_d\cos(\theta) - \tilde{w}_d\sin(\theta)] = 0. \end{aligned} \tag{41}$$

$$\begin{aligned} -E_d I_{zz}\frac{\mathrm{d}^4 \tilde{v}_d}{\mathrm{d}x^4} + F_x\left(\frac{\mathrm{d}^2 \tilde{v}_d}{\mathrm{d}x^2} - \eta^2\frac{\mathrm{d}^4 \tilde{v}_d}{\mathrm{d}x^4}\right) \\ +\left(1-\eta^2\frac{\mathrm{d}^2}{\mathrm{d}x^2}\right)Rc_d\left(\int_0^{2\pi} \tilde{w}\cos(\theta)\,\mathrm{d}\theta, -\pi\tilde{v}_d\right) = 0, \end{aligned} \tag{42}$$

$$\begin{aligned} -E_d I_{yy}\frac{\mathrm{d}^4 \tilde{w}_d}{\mathrm{d}x^4} + F_x\left(\frac{\mathrm{d}^2 \tilde{w}_d}{\mathrm{d}x^2} - \eta^2\frac{\mathrm{d}^4 \tilde{w}_d}{\mathrm{d}x^4}\right) \\ +\left(1-\eta^2\frac{\mathrm{d}^2}{\mathrm{d}x^2}\right)Rc_d\left(\int_0^{2\pi} \tilde{w}\sin(\theta)\,\mathrm{d}\theta, -\pi\tilde{w}_d\right) = 0. \end{aligned} \tag{43}$$

If the hybrid structure is subjected just to radial external pressure p_{ext} , the axial, normal and shear stresses in SWCNT vanish. The circumferential normal stresses occur only due to the vdW pressure from ssDNA exerted on the CNT. The axial, shearing and circumferential resultant forces are given by

$$N_x = 0, \tag{44a}$$

$$N_{x\theta} = 0, \tag{44b}$$

$$N_\theta = R(-p_{ext} + p_0). \tag{44c}$$

Substituting resultant forces into ψ from Eqn. (16) we get

$$\Psi = R(-p_{ext} + p_0)\frac{1}{R^2}\frac{\partial^2}{\partial\theta^2}. \tag{45}$$

Further substituting ψ into Eqn. (43), the equation governing the stability of ssDNA@SWCNT under radial pressure becomes

$$\begin{aligned} D\nabla^8\tilde{w}+\frac{Eh}{R^2}\frac{\partial^4\tilde{w}}{\partial x^4} \\ -(1-\eta^2\nabla^2)\nabla^4 R(-p_{ext}+p_0)\frac{1}{R^2}\frac{\partial^2}{\partial\theta^2}\tilde{w} \\ +(1-\eta^2\nabla^2)\nabla^4 c_d\left[\tilde{w}-\tilde{v}_d-\tilde{w}_d\right]=0 \end{aligned} \tag{46}$$

along with Eqns. (42, 43). Next, consider the following Ansatz solution for perturbation functions:

$$\tilde{w}=\tilde{W}\sin(m\pi x/L)sin(n\theta), \tag{47a}$$
$$\tilde{v}_d=\tilde{V}_d\sin(m\pi x/L), \tag{47b}$$
$$\tilde{w}_d=\tilde{W}_d\sin(m\pi x/L), \tag{47c}$$

where m and n are two non-negative integer representing the axial half wave-number and circumferential wave-number, and $\tilde{W}$, $\tilde{V}_d$ and $\tilde{W}_d$ are infinitesimal amplitudes of perturbation functions for the buckling mode corresponding to (m,n). Let us define following two parameters α and β:

$$\alpha=\frac{m\pi x}{L},\quad \beta=\frac{n}{R}. \tag{48}$$

Substituting Ansatz solution, Eqn. (47) into Eqns. (46, 42, 43) for circumferential mode $n=1$, we get

$$\begin{aligned} \Big(D(\alpha^2+\beta^2)^4+\frac{Eh}{R^2}+\left[1+\eta^2(\alpha^2+\beta^2)\right]\times\dots \\ (\alpha^2+\beta^2)^2R\beta^2(-p_{ext}+p_0)\tilde{W}+\left[1+\eta^2(\alpha^2+\beta^2)\right]\times\dots \\ (\alpha^2+\beta^2)^2c_d\left(\tilde{W}-\tilde{W}_d\right)\Big)\sin(\alpha x)\sin(\theta) \\ -(1+\eta^2)(\alpha^2+\beta^2)(\alpha^2+\beta^2)^2\times\dots \\ c_d(\tilde{V}_d)\sin(\alpha x)\cos(\theta)=0 \end{aligned} \tag{49}$$

$$\left(E_dI_{zz}\alpha^4+\pi Rc_d\eta^2\alpha^2+\pi Rc_d\right)\tilde{V}_d\sin(\alpha x)=0, \tag{50}$$

$$\begin{aligned} \left(E_dI_{yy}\alpha^4+\pi Rc_d\eta^2\alpha^2+\pi Rc_d\right)\tilde{W}_d\sin(\alpha x) \\ =\pi Rc_d(1+\eta^2\alpha^2)\tilde{W}sin(\alpha x), \end{aligned} \tag{51}$$

and also for $n\neq 0$,

$$\begin{aligned} \Big(D(\alpha^2+\beta^2)^4+\frac{Eh}{R^2}+\left[1+\eta^2(\alpha^2+\beta^2)\right]\times\dots \\ (\alpha^2+\beta^2)^2R\beta^2(-p_{ext}+p_0)\tilde{W}+\left[1+\eta^2(\alpha^2+\beta^2)\right]\times\dots \\ \dots(\alpha^2+\beta^2)^2c_d\Big)\tilde{W}\sin(\alpha x)\sin(\theta)=0. \end{aligned} \tag{52}$$

Eqns. (49-51, 52) are satisfied in the entire domain $0\leq x\leq L$ and $0\leq\theta\leq 2\pi$ (for $n=1$) if

$$\tilde{V}_d=0, \tag{53}$$

$$\begin{aligned} \left(E_dI_{yy}\alpha^4+\pi Rc_d\eta^2\alpha^2+\pi Rc_d\right)\tilde{W}_d \\ =\pi Rc_d(1+\eta^2\alpha^2)\tilde{W}, \end{aligned} \tag{54}$$

$$\begin{aligned} \Big(D(\alpha^2+\beta^2)^4+\frac{Eh}{R^2}+\left[1+\eta^2(\alpha^2+\beta^2)\right]\times\dots \\ (\alpha^2+\beta^2)^2R\beta^2(-p_{ext}+p_0)\tilde{W}+\left[1+\eta^2(\alpha^2+\beta^2)\right]\times\dots \\ (\alpha^2+\beta^2)^2c_d\left(\tilde{W}-\tilde{W}_d\right)\Big)=0, \end{aligned} \tag{55}$$

and for $n\neq 1$ if

$$\begin{aligned} \Big(D(\alpha^2+\beta^2)^4+\frac{Eh}{R^2}+\left[1+\eta^2(\alpha^2+\beta^2)\right]\times\dots \\ (\alpha^2+\beta^2)^2R\beta^2(-p_{ext}+p_0)+\left[1+\eta^2(\alpha^2+\beta^2)\right]\times\dots \\ (\alpha^2+\beta^2)^2c_d\Big)\tilde{W}=0. \end{aligned} \tag{56}$$

These algebraic equations governing the stability of ssDNA@SWCNT can be assembled into matrix form as

$$\begin{bmatrix}a_{11} & a_{12}\\ a_{21} & a_{22}\end{bmatrix}\begin{pmatrix}\tilde{W}\\ \tilde{W}_d\end{pmatrix}-p_{ext}\begin{bmatrix}b_{11} & 0\\ 0 & 0\end{bmatrix}\begin{pmatrix}\tilde{W}\\ \tilde{W}_d\end{pmatrix}=0, \tag{57}$$

where a_{ij} and b_{11} are given by

$$\begin{aligned} a_{11}=D(\alpha^2+\beta^2)^4+\frac{Eh}{R^2}+\left[1+\eta^2(\alpha^2+\beta^2)\right]\times\dots \\ (\alpha^2+\beta^2)^2\left(R\beta^2p_0+c_d\right) \end{aligned} \tag{58a}$$

$$a_{12}=-\left[1+\eta^2\left(\alpha^2+\beta^2\right)\right]\left(\alpha^2+\beta^2\right)^2c_d, \tag{58b}$$

$$a_{21}=-\pi Rc_d\left(1+\eta^2\alpha^2\right), \tag{58c}$$

$$a_{22}=E_dI_{yy}\alpha^4+\pi Rc_d\eta^2\alpha^2+\pi Rc_d, \tag{58d}$$

$$b_{11}=\left[1+\eta^2\left(\alpha^2+\beta^2\right)\right]\left(\alpha^2+\beta^2\right)^2R\beta^2. \tag{58e}$$

Following Eqn. (56), for circumferential modes corresponding to $n\neq 1$, the stability of the hybrid structure is governed by

$$\left(a_{11}-p_{ext}b_{11}\right)\tilde{W}=0,. \tag{59}$$

For existence of nontrivial solution for $(\tilde{W},\tilde{W}_d)$ in Eqn. (57) and for $\tilde{W}$ in Eqn. (59), the following condition must be satisfied:

$$p_{ext}=\begin{cases}\frac{a_{11}}{b_{11}}-\frac{a_{12}a_{21}}{a_{22}b_{11}} & \text{if } n=1,\\ \frac{a_{11}}{b_{11}} & \text{if } n\neq 1.\end{cases} \tag{60}$$

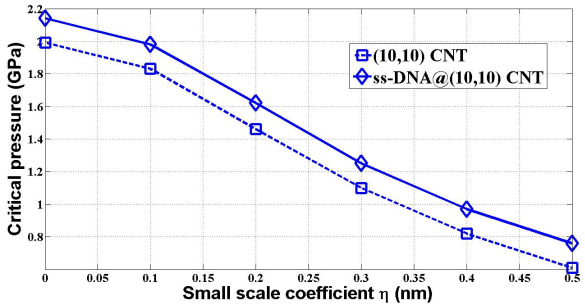

FIGURE 2. The critical pressure of pristine (10,10) CNT and the hybrid SSDNA@(10,10) CNT versus the small scale coefficient η.

The critical pressure at the onset of instability of ssDNA@SWCNT is minimimum p_{ext} for all axial and circumferential buckling modes (m,n).

6. NUMERICAL RESULTS AND DISCUSSION

Now, we provide numerical examples to obtain the critical radial pressure of the hybrid structure ssDNA@(10,10) CNT using nonlocal elastic rod and shell models. Based on MD simulations, Gao et al. [5] has reported that ssDNA can be inserted and encapsulated simultaneously inside (10,10) CNT with length of 5.9 nm due to the vdW inter-atomic interaction [5, 6]. The numerical values used for mechanical parameters here, for (10,10) CNT and also for ssDNA are $D = 0.85$ eV, $Eh = 360$ Jm^{-2} [53], $R = 0.678$ nm and $E_d = 100$ MPa [54,55]. The initial vdW pressure $p_0 = 0.1$ GPa and vdW interaction coefficient between ssDNA and SWCNT, is obtained as $c_d = 0.3$ GPa/nm from data in [6]. Now, we investigate the effect of filling a (10,10) CNT by a single-strand DNA on the radial instability of the unoccupied CNT. The length of the CNT and encapsulated ssDNA is assumed to be $L = 5.9$ nm, which is extracted from [5, 6]. The critical radial pressure for pristine (10,10) CNT and the hybrid ssDNA@(10,10) for a common range of η, i.e. the range below 1 nm for CNTs [49, 51] are plotted in Fig. 2. From Fig. 2, we see that the presence of the encapsulated ssDNA inside the (10,10) CNT results in an increase in the critical radial pressure. This means that the functionalized (10,10) CNT with ssDNA is stiffer and the resistance to the radial instability is enhanced by encapsulation of ssDNA. We have also seen similar increase in critical torque and critical axial force under the the effect of encapsulation of ssDNA into CNT. Although the formulation and the results are not provided here, one can readily confirm this fact by using appropriate resultant forces in Eqn. (44). For example, when CNT is subjected to external torque T, the resultant forces are

$$N_x = 0, \tag{61a}$$

$$N_{x\theta} = \frac{T}{2\pi R^2}, \tag{61b}$$

$$N_\theta = R(-p_{ext} + p_0). \tag{61c}$$

A similar increase of the resistance to the buckling instability of CNT due to encapsulation of some molecules and nanostructures has been reported in literature. For instance, due to the insertion of linear carbon chain (C-chain), the critical pressure and critical torsional moment of carbon nanowires, i.e. the functionalized CNT with linear carbon chain encapsulated inside CNT [4,9], have been reported to be larger than the pristine CNT of radius around 0.35nm such as (5,5) or (9,0) CNT [20]. Furthermore, encapsulation of C_{60} fullerenes inside CNT leads to a new category of hybrid CNTs called carbon nano-peapods. It has been reported that the encapsulation of C_{60} fullerenes inside (10,10) CNT results in an increase of the resistance to buckling instability of (10,10) CNT under axial compressive force [14], torsional moment [15,17], bending moment [17]) and radial pressure [18]. In both cases of nano-wires with innermost CNT radius of 0.35nm and C_{60}@(10,10) nano-peapods, the encapsulation process has been reported to occur spontaneously. This is because of the fact that the host CNT in the mentioned range of diameters makes a proper space for the nested C_{60} fullerenes or carbon chain to maintain a preferred graphitic van der Waals (vdW) separation (i.e. 0.3nm) from the interior wall of CNT [3].The insertion and encapsulation of ssDNA inside (10,10) CNT with length of 5.9nm has been reported to be a spontaneous process and the hybrid ssDNA@(10,10) is energetically more stable [5, 6]. Therefore, similar to C_{60}@(10,10) carbon nano-peapods and C-chain@(5,5) or C-chain@(9,0) carbon nanowires, an increase in resistance to radial buckling for ssDNA@(10,10) CNT is not surprising.

Finally, we note from Fig. 2 that the critical pressures of pristine (10,10) CNT and ssDNA@(10,10) for small scale coefficient $\eta = 0.15$ nm are computed to be 1.65 GPa and 1.8 GPa respectively. This implies an increase of about 10% in buckling strength of (10,10) CNT under radial pressure due to the encapsulation of ssDNA.

7. CONCLUSIONS

This paper contributes a model for buckling analysis of hybrid CNTs functionalized by encapsulation of single-stranded DNA by introducing nonlocal elasticity in shell model for CNT and rod model for ssDNA. The model predicts that the encapsulation increases resistance to buckling and that the nonlocal elasticity theory predicts lower critical pressure than does the local elasticity theory.

REFERENCES

[1] Iijima, S., 1991. "Helical microtubules of graphitic carbon". *Nature,* ***354***(6348), pp. 56–58.

[2] Cole, M. W., Crespi, V. H., Stan, G., Ebner, C., Hartman, J. M., Moroni, S., and Boninsegni, M., 2000. "Condensation of helium in nanotube bundles". *Phys. Rev. Lett.,* ***84***(17), pp. 3883–3886.

[3] Smith, B., Monthioux, M., and Luzzi, D., 1999. "Carbon nanotube encapsulated fullerenes: a unique class of hybrid materials". *Chem. Phys. Lett.,* ***315***(1-2), pp. 31–36.

[4] Wang, Z., Ke, X., Zhu, Z., Zhang, F., Ruan, M., and Yang, J., 2000. "Carbon-atom chain formation in the core of nanotubes". *Phys. Rev. B,* ***61***, pp. R2472–R2474.

[5] Gao, H., Kong, Y., Cui, D., and Ozkan, C. S., 2003. "Spontaneous insertion of DNA oligonucleotides into carbon nanotubes". *Nano. Lett.,* ***3***(4), pp. 471–473.

[6] Gao, H., and Kong, Y., 2004. "Simulation of DNA-nanotube interactions". *Annu. Rev. Mater. Res.,* ***34***, pp. 123–150.

[7] Cui, D., Ozkan, C. S., Ravindran, S., Kong, Y., and Gao, H., 2004. "Encapsulation of pt-labelled dna molecules inside carbon nanotubes". *Mech. chem. Biosys.,* ***1***(2), pp. 113–121.

[8] Monthioux, M., 2002. "Filling single-wall carbon nanotubes". *Carbon,* ***40***(10), pp. 1809–1823.

[9] Zhao, X., Ando, Y., Liu, Y., Jinno, M., and Suzuki, T., 2003. "Carbon nanowire made of a long linear carbon chain inserted inside a multiwalled carbon nanotube". *Phys. Rev. Lett.,* ***90***(18), p. 187401.

[10] Li, J., Ng, H. T., Cassell, A., Fan, W., Chen, H., Ye, Q., Koehne, J., Han, J., and Meyyappan, M., 2003. "Carbon nanotube nanoelectrode array for ultrasensitive dna detection". *Nano Lett.,* ***3***(5), pp. 597–602.

[11] Qi, P., Vermesh, O., Grecu, M., Javey, A., Wang, Q., Dai, H., Peng, S., and Cho, K. J., 2003. "Toward large arrays of multiplex functionalized carbon nanotube sensors for highly sensitive and selective molecular detection". *Nano Lett.,* ***3***(3), pp. 347–351.

[12] Hamdi, M., and Ferreira, A., 2008. "DNA nanorobotics". *MICROELECTR. J.,* ***39***(8), pp. 1051–1059.

[13] Jeong, B.-W., Lim, J.-K., and Sinnott, S. B., 2007. "Elastic torsional responses of carbon nanotube systems". *J. Appl. Phys.,* ***101***(8), pp. 084309–7.

[14] Ni, B., Sinnott, S., Mikulski, P., and Harrisson, J., 2002. "Compression of carbon nanotubes filled with c60, ch4, or ne: Predictions from molecular dynamics simulations". *Phys. Rev. Lett.,* ***88***, pp. 205505–205508.

[15] Wang, Q., 2009. "Torsional instability of carbon nanotubes encapsulating c60 fullerenes". *Carbon,* ***47***, pp. 507–512.

[16] Zang, J., Alds-Palacios, O., and Liu, F., 2007. "Md simulation of structural and mechanical transformation of single-walled carbon nanotubes transformation of single-walled carbon nanotubes". *Commun. Comput. Phys.,* ***2***(3), pp. 451–465.

[17] Zhu, J., Pan, Z., Wang, Y., Zhou, L., and Jiang, Q., 2007. "The effects of encapsulating c60 fullerenes on the bending flexibility of carbon nanotubes". *Nanotechnology,* ***18***(27), p. 275702.

[18] Asghari, M., Naghdabadi, R., and Rafati-Heravi, J., 2011. "Small scale effects on the stability of carbon nano-peapods under radial pressure". *Phys. E,* ***43***(5), pp. 1050–1055.

[19] Asghari, M., Rafati, J., and Naghdabadi, R., 2013. "Torsional instability of carbon nano-peapods based on the nonlocal elastic shell theory". *Phys. E,* ***47***(0), pp. 316 – 323.

[20] Hu, Z., Guo, X., and Ru, C., 2008. "Enhanced critical pressure for buckling of carbon nanotubes due to an inserted linear carbon chain". *Nanotechnology,* ***19***(30), p. 305703.

[21] Song, H., Li, L., and Feng, F., 2009. "Torsional behaviour of carbon nanotubes with abnormal interlayer distances". *J. Phys. D.,* ***42***(5), p. 055414.

[22] He, X. Q., Kitipornchai, S., and Liew, K. M., 2005. "Buckling analysis of multi-walled carbon nanotubes: a continuum model accounting for van der waals interaction". *J. Mech. Phys. Solids,* ***53***(2).

[23] Kitipornchai, S., He, X. Q., and Liew, K. M., 2005. "Buckling analysis of triple-walled carbon nanotubes embedded in an elastic matrix". *J. Appl. Phys.,* ***97***(11), pp. 1–7.

[24] Ru, C., 2000. "Elastic buckling of single-walled carbon nanotube ropes under high pressure". *Phys. Rev. B,* ***62***, pp. 10405–10458.

[25] Yang, H. K., and Wang, X., 2006. "Bending stability of multi-wall carbon nanotubes embedded in an elastic medium". *Model. Simul. Mater. Sci. Eng.,* ***14***(1), pp. 99–116.

[26] Wang X., Y. H., and K., D., 2005. "Torsional buckling of multi-walled carbon nanotubes". *Mater. Sci. Eng. A,* ***404***(1-2).

[27] Goyal, S., Perkins, N. C., and Lee, C. L., 2003,. "Torsional buckling and writhing dynamics of elastic cables and DNA". *Proceedings of the ASME 2003 IDETC/CIE, Chicago, Illinois, USA.,* ***5***(Paper No. DETC2003/VIB-48322), pp. 183–191.

[28] Goyal, S., Perkins, N. C., and Lee, C. L., 2005. "Nonlinear dynamics and loop formation in kirchhoff rods with implications to the mechanics of dna and cables". *J. Comput. Phys.,* ***209***(1), pp. 371–389.

[29] Goyal, S., 2006. "A dynamic rod model to simulate mechanics of cables and dna". Ph.D. dissertation in mechanical engineering, University of Michigan.

[30] Balaeff, A., Mahadevan, L., and Schulten, K., 2006. "Modeling DNA Loops Using the Theory of Elasticity". *Physical Review E,* ***73***(3).

[31] Goyal, S., and Perkins, N., 2008. "Looping mechanics of rods and DNA with non-homogeneous and discontinuous

stiffness". *Int. J. .Nonlinear Mech.,* ***44***.

[32] Lillian, T., Goyal, S., Kahn, J. D., Meyhofer, E., and Perkins, N. C., 2008. "Computational Analysis of Looping of a Large Family of Highly Bent DNA by LacI". *Biophys. J.,* ***95***(12), pp. 5832–42.

[33] Goyal, S., Lillian, T., Blumberg, S., Meiners, J. C., Meyhofer, E., and Perkins, N. C., 2007. "Intrinsic Curvature of DNA Influences LacR-Mediated Looping". *Biophysical Journal,* ***93***(12), pp. 4342–4359.

[34] Goyal, S., Perkins, N., and Lee, C. L., 2008. "Non-linear dynamic intertwining of rods with self-contact". *Int. J. of Nonlinear Mech.,* ***43***(1), pp. 65–73.

[35] Goyal, S., Perkins, N. C., and Lee, C. L., 2003. "Writhing dynamics of cables with self-contact". pp. 27–36.

[36] Hinkle, A. R., Goyal, S., and Palanthandalam-Madapusi, H. J. "Constitutive-law modeling of microfilaments from their discrete-structure simulations-a method based on an inverse approach applied to a static rod model". *J. Appl. Mech.,* ***79***(5), p. 051005.

[37] Palanthandalam-Madapusi, H. J., and Goyal, S., 2011. "Robust estimation of nonlinear constitutive law from static equilibrium data for modeling the mechanics of DNA". *Automatica,* ***47***(6), pp. 1175–1182.

[38] Hinkle, A. R., Goyal, S., and Palanthandalam-Madapusi, H. J., 2009. "An Estimation Method of a Constitutive-law for the Rod Model of DNA using Discrete-Structure Simulations". *Proceedings of the ASME 2009 IDETC/CIE, San Diego, CA, USA.*

[39] Palanthandalam-Madapusi, H. J., and Goyal, S., 2008. "Estimation of Nonlinear Sequence-dependent Constituative Law for DNA Molecules". *47th IEEE Conference on Decision and Control, Cancun, Mexico, December.*, pp. 2674–2679.

[40] Eringen, A. C., 1972. "Nonlocal polar elastic continua". *Int. J. Eng. Sci.,* ***10***(1), pp. 1–16.

[41] Eringen, A., 1983. "On differential equations of nonlocal elasticity and solutions of screw dislocation and surface waves". *J. Appl. Phys.,* ***54***, pp. 4703–4710.

[42] Adali, S., 2009. "Variational principles for transversely vibrating multiwalled carbon nanotubes based on nonlocal euler-bernoulli beam model". *Nano Lett.,* ***9***(5), pp. 1737–1741.

[43] Aydogdu, M., 2009. "A general nonlocal beam theory: Its application to nanobeam bending, buckling and vibration". *Phys. E,* ***41***(9).

[44] Peddieson, J., Buchanan, G., and McNitt, R., 2003. "Application of nonlocal continuum models to nanotechnology". *Int. J. Eng. Sci.,* ***41***, p. 305312.

[45] Reddy, J. N., 2007. "Nonlocal theories for bending, buckling and vibration of beams". *Int. J. Eng. Sci.,* ***45***(2-8), pp. 288–307.

[46] Zhang, Y. Q., Liu, G. R., and Han, X., 2006. "Effect of small length scale on elastic buckling of multi-walled carbon nanotubes under radial pressure". *Phys. Lett. A,* ***349***(5), pp. 370–376.

[47] Zhang, Y., Liu, G., and Han, X., 2004. "Small-scale effects on buckling of multiwalled carbon nanotubes under axial compression". *Phys. Rev. B,* ***70***(20), pp. 1–7.

[48] Hao, M. J., Guo, X. M., and Wang, Q., 2009. "Small-scale effect on torsional buckling of multi-walled carbon nanotubes". *Eur. J. Mech. A-Solids,* ***29***(1), pp. 49–55.

[49] Li, R., and Kardomateas, G., 2007. "Thermal buckling of multi-walled carbon nanotubes by nonlocal elasticity". *ASME J. Appl. Mech.,* ***74***, pp. 399–405.

[50] Li, R., and Kardomateas, G. A., 2007. "Vibration characteristics of multiwalled carbon nanotubes embedded in elastic media by a nonlocal elastic shell model". *J. Appl. Mech.-T. ASME,* ***74***(6), pp. 1087–1094.

[51] Hu, Y.-G., Liew, K. M., Wang, Q., He, X. Q., and Yakobson, B. I., 2008. "Nonlocal shell model for elastic wave propagation in single- and double-walled carbon nanotubes". *J. Mech. Phys. Solids,* ***56***(12), pp. 3475–3485.

[52] Donnell, L., 1976. *Beams, Plates, and Shells.* McGraw-Hill, New York.

[53] Yakobson, B. I., Brabec, C. J., and Bernholc, J., 1996. "Nanomechanics of carbon tubes: Instabilities beyond linear response". *Phys. Rev. Lett.,* ***76***(14), pp. 2511–2514.

[54] Morii, T., Mizuno, R., Haruta, H., and Okada, T., 2004. "An afm study of the elasticity of dna molecules". *Thin Solid Films,* ***464-465***, pp. 456–458.

[55] Munteanu, M. G., Vlahovicek, K., Parthasarathy, S., Simon, I., and Pongor, S., 1998. "Rod models of dna: sequence-dependent anisotropic elastic modelling of local bending phenomena". *Trends Biochem. Sci.,* ***23***(9), pp. 341–347.